Int. J. Heat Mass Transfer. Vol. 33, No. 6, pp. 1165–1175, 1990
Printed in Great Britain

0017–9310/90 $3.00 + 0.00

Numerical study of steady state and transient laser melting problems—II. Effect of the process parameters

BISWAJIT BASU
Tata Research Development and Design Centre, 1, Mangaldas Road, Pune 411 001, India

and

A. W. DATE
Department of Mechanical Engineering, Indian Institute of Technology, Powai, Bombay 400 076, India

(*Received* 6 *September* 1988 *and in final form* 30 *January* 1989)

Abstract—A parametric study of laser melting problems is presented. Using steel ($Pr = 0.078$) and aluminium ($Pr = 0.01$), studies are made by varying beam radius (0.5, 1.0 and 2.0 mm) and beam power density (10^8–10^9 W m^{-2}). The effects of these parameters are studied on the bulk mean temperature of the liquid, the maximum width and depth of the pool, the area of the solid/liquid interface, the area of the liquid phase and the interface Nusselt number. Comparative studies are performed between pure conduction and convection cases to analyse the effect of convection on the overall heat transfer, and thus the critical values of process parameters are identified below which convection is negligible. The maximum pool width is found to be invariant for beams of varying radii when the product of beam power and radius is constant. Finally, correlations are derived to determine the bulk mean temperature of the liquid, the maximum width and depth of the pool and the interface Nusselt number from the process parameters.

1. INTRODUCTION

FLUID FLOW plays a major role during laser melting [1–4] and thus controls the total heat transfer under certain combinations of power density and radius of the beam [4]. The flow pattern in the molten pool shows the existence of two contra-rotating cells [4] which influence the total heat transfer. From the paper of Basu and Date [4], it is very clear that the pool shape is controlled by complex heat transfer phenomena—conduction and primary and secondary convection. Though it is understood that convective heat transfer plays a dominant role, the onset of convection in the pool and, subsequently, its dominance over conduction heat transfer has not yet been studied as a function of the process parameters. All previous studies [1–4] were directed to analyse the flow pattern and heat transfer for some specific cases. A parametric study of laser melting for a wide range of process parameters to analyse the nature of the pool geometry is also of considerable importance.

The process parameters for laser melting are beam power density, beam radius and materials. In this paper, the effect of these parameters on the depth, width and area of the pool and on the interface area are studied. The effect of convection on the total heat transfer is demonstrated through the variation of two dependent variables:

(a) interface Nusselt number (Nu_1) and
(b) bulk mean temperature of the liquid (θ_{bulk}).

The onset of convection and its relative dominance over conduction are clearly demonstrated through the variation of these two parameters for the cases of (a) pure conduction and (b) convection.

2. NUMERICAL SIMULATION

The physical problem, along with the assumptions and mathematical formulation, are described in detail by Basu and Date [4].

The effect of process parameters are studied with the help of a wide range of values of the non-dimensional numbers. These are:

$$Ma = \text{Marangoni number} = \frac{U_R r_0}{\alpha}$$

$$Pr = \text{Prandtl number} = \frac{\nu}{\alpha}$$

$$B_f = \text{boundary heating number} = \frac{q'' r_0 C_{pl}}{K_l \lambda}$$

and

$$Ste = \text{Stefan number} = \frac{C_{ps}(T_m - T_\infty)}{\lambda}.$$

NOMENCLATURE

A_I	normalized area of the interface
A_l	normalized area of the molten pool
B_f	boundary heating factor, $q'' r_0 C_{pl}/k_l \lambda$
C_p	specific heat [J kg^{-1} K^{-1}]
h_I	heat transfer coefficient at the interface [W m^{-1} K^{-1}]
K	thermal conductivity [W m^{-1} K^{-1}]
l_r	length along the constant r
l_z	length along the constant z
Nu	Nusselt number, hr_0/k
Ma	Marangoni number, $U_R r_0/\alpha$
Pr	Prandtl number, ν/α
q''	beam power density [W m^{-2}]
q_I	heat flux at the interface [W]
R_σ	surface tension Reynolds number, $U_R r_0/\nu$
r_0	beam radius [m]
r_{max}	maximum width of the molten pool
Ste	Stefan number, $C_p(T_m - T_\infty)/\lambda$
T	temperature [K]
U_R	surface tension reference velocity, $(d\sigma/dT) \cdot \lambda/(C_{pl}\mu)$
z_{max}	maximum width of the molten pool.

Greek symbols

α	thermal diffusivity [m^2 s^{-1}]
θ_{bulk}	bulk mean temperature of the liquid
λ	latent heat of fusion [J kg^{-1}]
ν	kinematic viscosity [m^2 s^{-1}].

Subscripts

I	interface
l	liquid
s	solid
ss	steady state.

Superscript

*	dimensional value.

2.1. *Definition of Nu_I and θ_{bulk}*

If h_I is the average heat transfer coefficient at the interface, the total heat transfer through the solid/liquid interface can be written as

$$\int_{A_I} q_I^* \, dA = h_I A_I (T_{bulk} - T_m). \quad (1)$$

Normalizing this equation in the same way as mentioned by Basu and Date [4], the interface Nusselt number is given by

$$Nu_I = \frac{h_I r_0}{K} = \frac{\int_{A_I} q_I \, dA}{A_I \theta_{bulk}} \quad (2)$$

where

$$\theta_{bulk} = \frac{1}{A_l} \int_{A_l} \theta \, dA. \quad (3)$$

Under steady state conditions $\int_{A_I} q_I \, dA$ is equal to the net heat input from the top boundary, hence

$$Nu_{Iss} = \frac{B_f \int_0^1 r \exp(-2r^2) \, dr}{A_l \theta_{bulk}}. \quad (4)$$

The total molten area A_l is determined in the following way:

$$A_l = \int_r \int_z r \, dr \, dz|_{liquid} \quad (5)$$

and the total interfacial area (A_I) is calculated as follows:

$$A_I = \int_{l_z} r \, dr \, (\text{along constant } z) + \int_{l_r} r \, dz \, (\text{along constant } r) \quad (6)$$

where l_z and l_r are the lengths along the constant z and r directions, respectively.

The numerical description along with the typical grid distribution is given by Basu and Date [4]; (24 × 24) grids were used for the parametric study. One steady state run takes around 18 min on the ELXSI 6400 computer.

3. RESULTS AND DISCUSSION

Results are presented for two materials, aluminium ($Pr = 0.01$ and $Ste = 1.6732$) and steel ($Pr = 0.078$ and $Ste = 3.2516$), for different values of non-dimensional numbers as follows.

Aluminium

$Ma = 1728$–6912 ($r_0 = 0.5$–2.0 mm),

$B_f = 10$–40 ($q'' = 10^8$–10^9 W m^{-2}).

Steel

$Ma = 491.5$–1806.0 ($r_0 = 0.5$–2.0 mm),

$B_f = 20$–50 ($q'' = 10^8$–10^9 W m^{-2}).

Parametric studies are presented for the following variables:

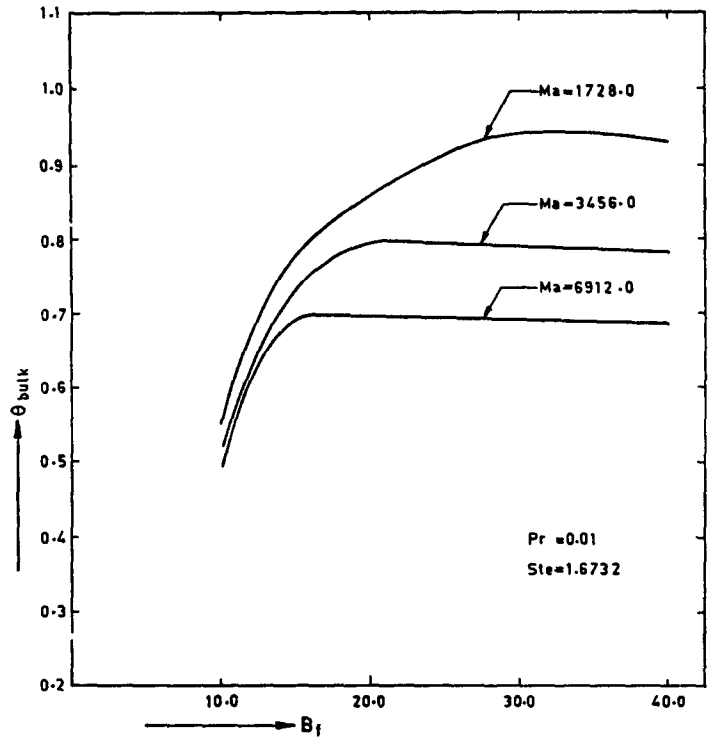

FIG. 1. Variation of bulk mean temperature (θ_{bulk}) with Marangoni number (Ma) and boundary heating factor (B_f) for aluminium.

θ_{bulk} = bulk mean temperature of the liquid, equation (3)
r_{max} = maximum width of the pool
z_{max} = maximum depth of the pool
A_l = total area of the molten pool, equation (5)
A_i = total interfacial area, equation (6)

and

Nu_i = interface Nusselt number, equations (4) and (2).

Finally correlations of θ_{bulk}, r_{max}, z_{max} and Nu_{iss} are presented as:

$$\theta_{bulk}, r_{max}, z_{max} \quad \text{and} \quad Nu_{iss} = f(Ma, B_f, Ste).$$

3.1. *Steady state analysis*

3.1.1. *Bulk mean temperature* (θ_{bulk}). Figure 1 shows the effect of Ma and B_f on the bulk mean temperature (θ_{bulk}) for aluminium. For a given material (i.e. fixed Pr and Ste), Ma is directly proportional to the beam radius, whereas B_f is directly proportional to the product of the beam radius and the beam power. θ_{bulk} increases sharply with B_f up to a certain value and then decreases slowly. The value of θ_{bulk} decreases with Ma for a fixed B_f. At low B_f (i.e. $B_f = 10.0$), θ_{bulk} values for all Ma are seen to converge, indicating dominance of conduction heat transfer. At low values of B_f, convection cannot play a dominant role because of the smaller pool dimension, resulting in high viscous force which suppresses fluid flow. Before explaining the trend of θ_{bulk}, it is important to note the θ_{bulk} variation in comparison to pure conduction; Fig. 2 shows the comparative study of θ_{bulk} without and with ($Ma = 6912$) convection for aluminium. The θ_{bulk} with conduction increases steadily with B_f, whereas θ_{bulk} with convection decreases after reaching a maximum value (i.e. at $B_f = 20.0$). At higher B_f values, there is a strong convection which results in better mixing and thus reduces the bulk temperature level. At lower B_f values convection is not strong enough and θ_{bulk} increases because of dominant conduction heat transfer. The difference between θ_{bulk} with and without convection increases with increasing B_f when convection starts playing the dominant role. It can therefore be concluded that convection starts playing a role when B_f is 10.0 for aluminium and dominates over conduction heat transfer for $B_f = 20.0$. The trend of θ_{bulk} (Fig. 1) is now clear. For higher Ma values, the convective heat transfer is more dominant than with lower Ma values. As a result, θ_{bulk} with lower Ma values is higher than that of higher Ma.

The θ_{bulk} variation of steel with B_f for different values of Ma is shown in Fig. 3. The trend of results is the same as those for aluminium except that θ_{bulk} decreases at a faster rate for higher values of B_f. The Prandtl number of steel (0.078) is higher than that of aluminium (0.01) and this results in a more dominant role for convection. Figure 4 shows a comparison

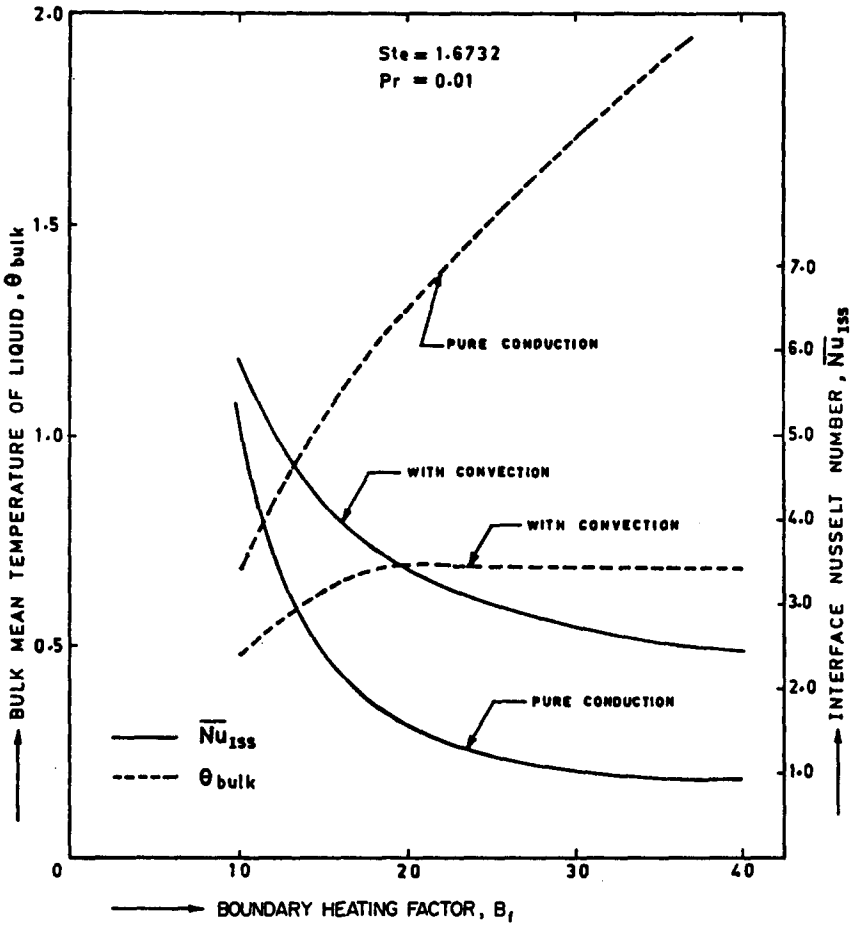

FIG. 2. Comparison of variation of interface Nusselt number (Nu_{1ss}) and bulk mean temperature (θ_{bulk}) with boundary heating factor (B_f) between pure conduction and convection with $Ma = 6912.0$ for aluminium.

of θ_{bulk} with ($Ma = 1806.0$) and without convection. Convection starts playing a role when B_f is 20.0 and dominates over conduction for $B_f \geqslant 30$ (Fig. 4). The critical B_f is higher for steel ($Ste = 3.2516$) than for aluminium ($Ste = 1.6732$) because of the high Stefan number of steel, which represents a higher rate of sensible heat transfer before melting starts.

3.1.2. *Steady state interface Nusselt number, Nu_{1ss}.* Reference to Figs. 2 and 4 shows that steady state Nusselt numbers, Nu_{1ss}, with convection are always greater than those without convection; the difference between the two increases with increasing B_f. This trend further confirms the importance of convection in laser melting.

Figures 5 and 6 show the Nu_{1ss} variation with convection for different Ma values. For aluminium and steel, the Nu_{1ss} at small B_f are considerably larger because of the small interfacial area A_1 (see Figs. 9 and 10) and small θ_{bulk}. As B_f is increased, θ_{bulk} and A_1 increase, leading to an overall decline in the values of Nu_{1ss}. However, this conclusion appears to be true only for aluminium, which has a low Pr value. For steel, a small increase in Nu_{1ss} is observed at large B_f because θ_{bulk}, after increasing with B_f, begins to fall (see Fig. 3) beyond a B_f value of 30. Nu_{1ss} would thus have increased sharply with B_f if it were not for the sharp increase in A_1 at higher B_f values (see Fig. 10).

3.1.3. *Maximum width (r_{max}) and depth (z_{max}) of the pool.* The variations of r_{max} and z_{max} for aluminium and steel are shown in Figs. 7 and 8, respectively. For a given material, the predicted r_{max} (i.e. the normalized width of the pool) values are seen to be independent of Ma (i.e. the beam radius, r_0) for fixed B_f, which is proportional to the product of q and r_0. The predicted depth of the pool (i.e. z_{max}) on the other hand is seen to be a function of both Ma and B_f. These results are of considerable importance from the engineering point of view. They lead to the determination of the beam scanning width and to the choice of the beam power and beam radius for a desired melt depth.

3.1.4. *Total molten area (A_1) and interfacial area (A_1).* The variations of A_1 and A_1 with Ma and B_f for aluminium and steel are shown in Figs. 9 and 10, respectively. It is again interesting to note the small variation of both A_1 and A_1 under different conditions. In fact the maximum variations of A_1 and A_1 are 10 and 15%, respectively. Again both A_1 and A_1 for different Ma values converge at low values of B_f, showing the dominance of conduction heat transfer. The variations of A_1 and A_1 for different Ma values

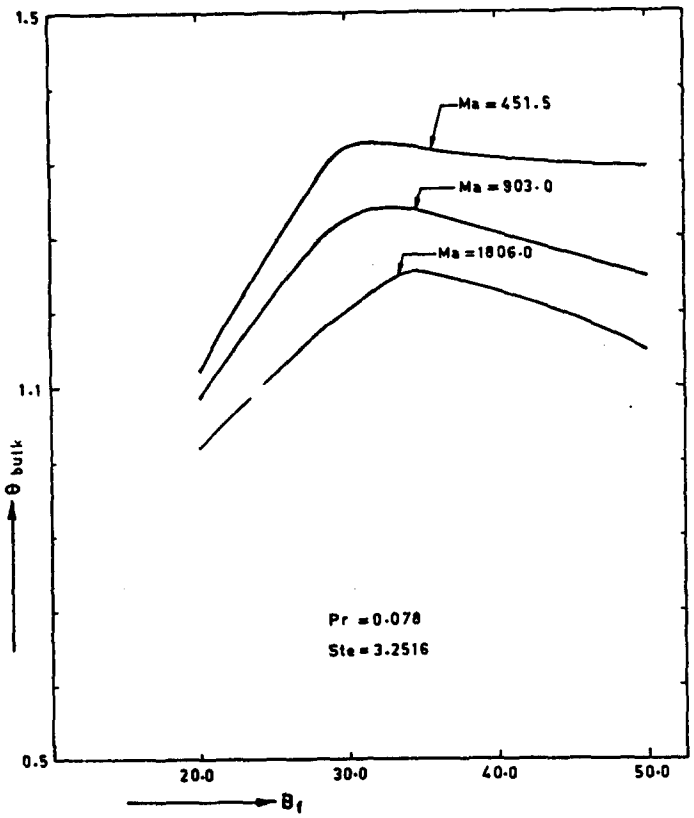

FIG. 3. Variation of bulk mean temperature (θ_{bulk}) with Marangoni number (Ma) and boundary heating factor (B_f) for steel.

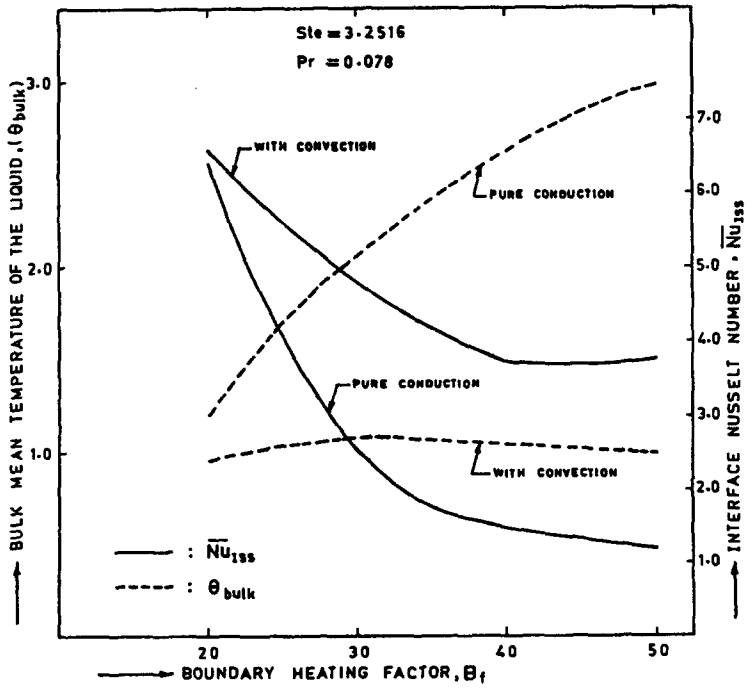

FIG. 4. Comparison of variation of interface Nusselt number (Nu_{1ss}) and bulk mean temperature (θ_{bulk}) with boundary heating factor (B_f) between pure conduction and convection with Ma = 1806.0 for steel.

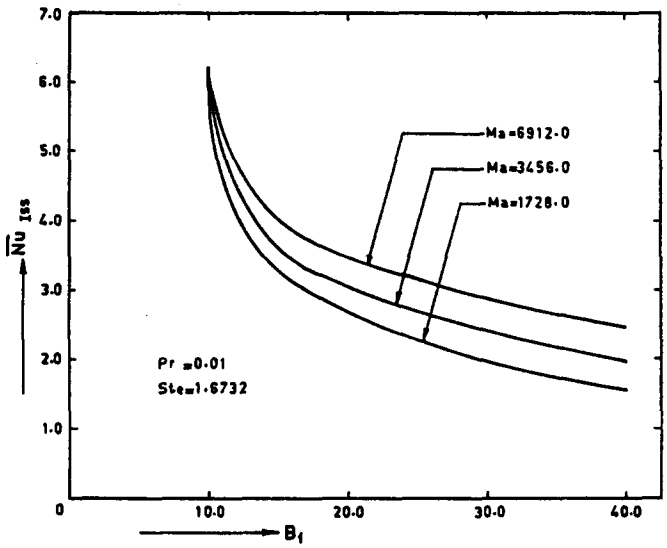

FIG. 5. Variation of steady state interface Nusselt number (Nu_{iss}) with Marangoni number (Ma) and boundary heating factor (B_f) for aluminium.

arise because of the difference in z_{max}, which in turn is influenced by the secondary cells.

3.1.5. *Correlations.* From the engineering point of view, the important parameters for laser surface treatment are θ_{bulk}, r_{max}, z_{max} and Nu_{iss}. θ_{bulk} signifies the superheat level in the molten pool and it is important to maintain lower superheat from the point of view of rapid solidification. The scanning width and depth of the heat affected zone are represented by r_{max} and z_{max}, respectively; these inputs are required for carrying out any laser surface treatment where heat affected depth is specified. Finally, the role of convection can be determined from the variation of Nu_{iss}. Realizing the importance of all these parameters, the following correlations are derived as a function of the process parameters.

For aluminium ($Pr = 0.01$ and $Ste = 1.6732$)

$$\theta_{bulk} = 1.067\,(Ma)^{-0.1732}(B_f)^{0.3243}$$

$$r_{max} = 0.154\,(B_f)^{0.7519}$$

$$z_{max} = 0.089\,(Ma)^{-0.1}(B_f)^{1.0415}$$

$$Nu_{iss} = 6.6587\,(Ma)^{0.215}(B_f)^{-0.823}.$$

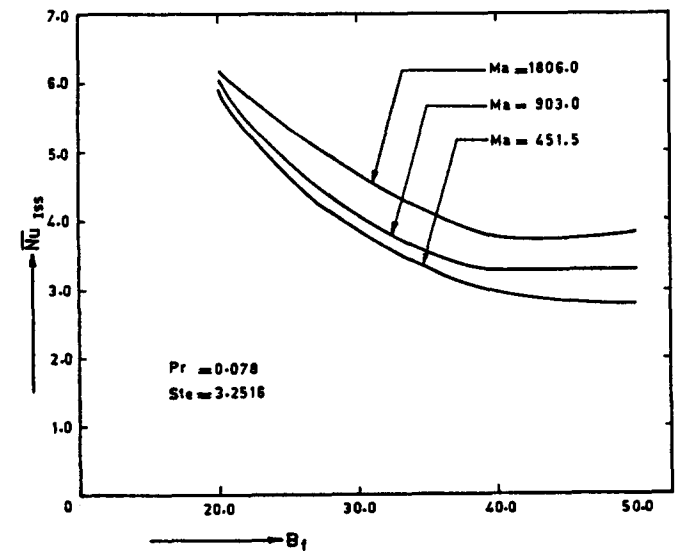

FIG. 6. Variation of steady state interface Nusselt number (Nu_{iss}) with Marangoni number (Ma) and boundary heating factor (B_f) for steel.

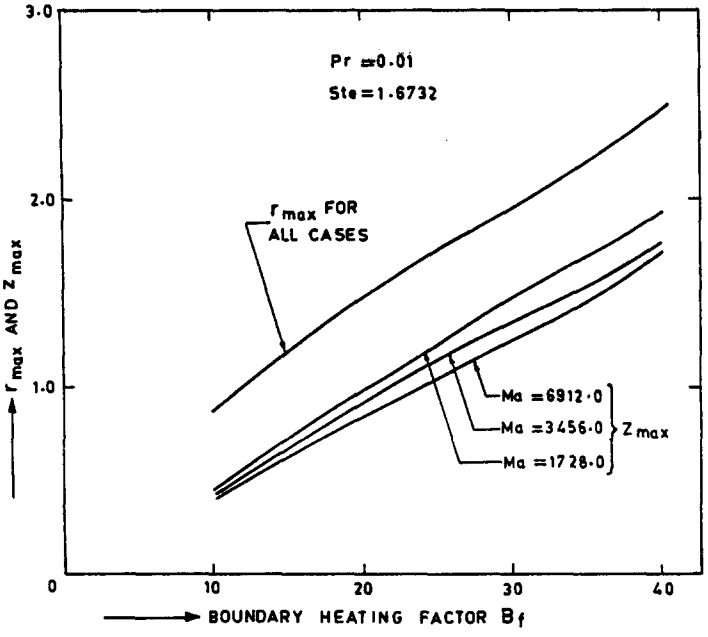

FIG. 7. Variation of r_{max} and z_{max} with Marangoni number (Ma) and boundary heating factor (B_f) for aluminium.

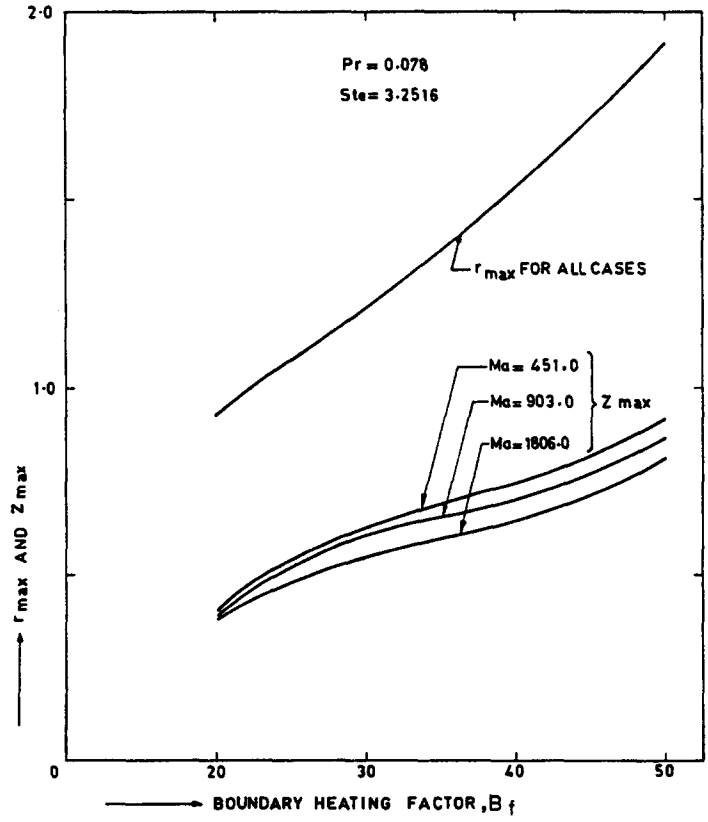

FIG. 8. Variation of r_{max} and z_{max} with Marangoni number (Ma) and boundary heating factor (B_f) for steel.

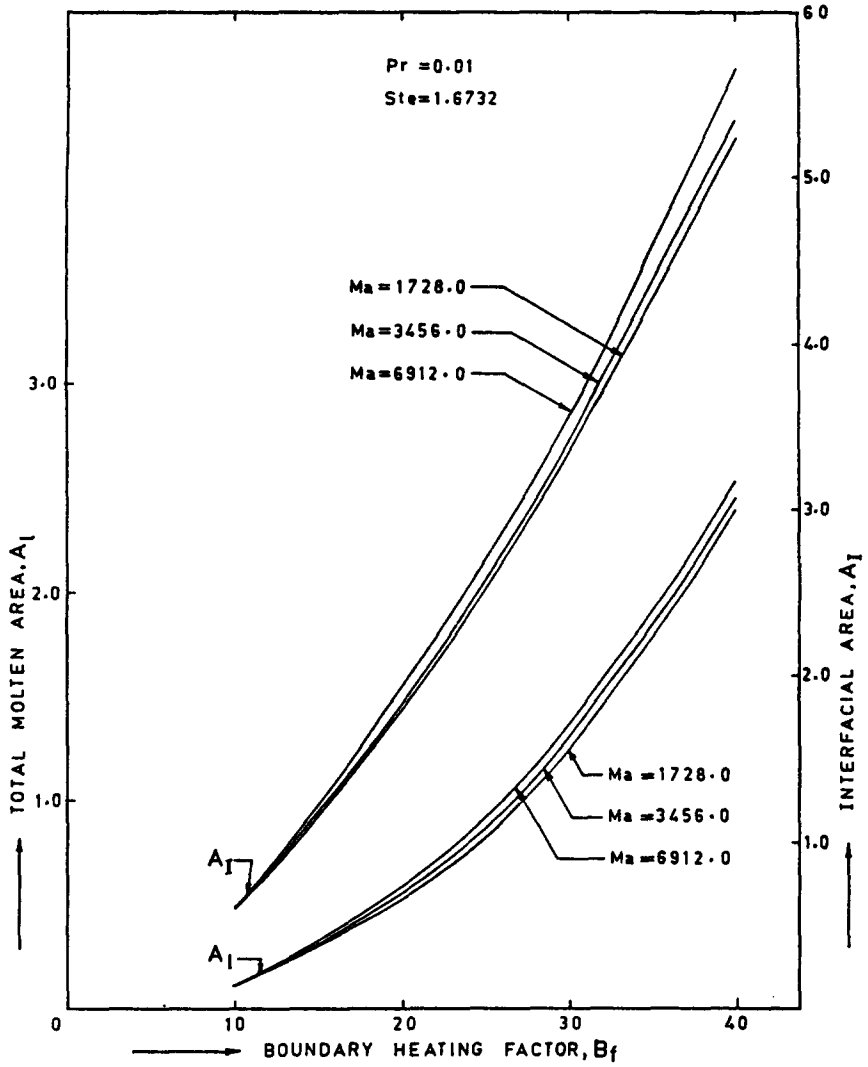

FIG. 9. Variation of total molten area (A_l) and interfacial area (A_I) with Marangoni number (Ma) and boundary heating factor (B_f) for aluminium.

For steel ($Pr = 0.078$ and $Ste = 3.2516$)

$$\theta_{bulk} = 1.276\,(Ma)^{-0.1186}(B_f)^{-0.1968}$$

$$r_{max} = 0.0865\,(B_f)^{0.7856}$$

$$z_{max} = 0.0607\,(Ma)^{-0.086}(B_f)^{0.829}$$

$$Nu_{Iss} = 18.323\,(Ma)^{0.1679}(B_f)^{-0.7487}.$$

3.2. *Transient study*

Figures 11 and 12 show the transient development of Nu_I, r_{max} and z_{max} for aluminium and steel, respectively, for a beam of 4×10^8 W m^{-2} and 2 mm radius; the values of the non-dimensional parameters are given in the figures. The interface Nusselt number (Nu_I) falls very fast during the initial transient and asymptotically approaches its steady state value. During the initial stage of melting, when the pool size is smaller, conduction is the dominant mode of heat transfer and this results in a fast increase of θ_{bulk} due to accumulation of heat. On the other hand, both interface heat transfer (q_I) and interfacial area (A_I) are small. This results in a sharp decrease in Nu_I during the initial stages of melting. After the initial transient, both q_I and A_I increase and the rate of increase of θ_{bulk} decreases because of better mixing due to convection. As a result, Nu_I decreases slowly to reach its steady state value.

r_{max} increases very fast during the initial transient. While comparing the r_{max} development between aluminium and steel, it can be seen that the time for the interface to reach the edge of the beam (i.e. $r = 1.0$) is 0.5 for aluminium and 0.9 for steel, but these times correspond to different scales and they are 0.1 and 0.9 respectively in terms of the steel time scale for aluminium and steel. The onset of melting for aluminium is earlier than that of steel because of lower sensible heat removal for aluminium before melting. z_{max} (which is commonly known as penetration depth)

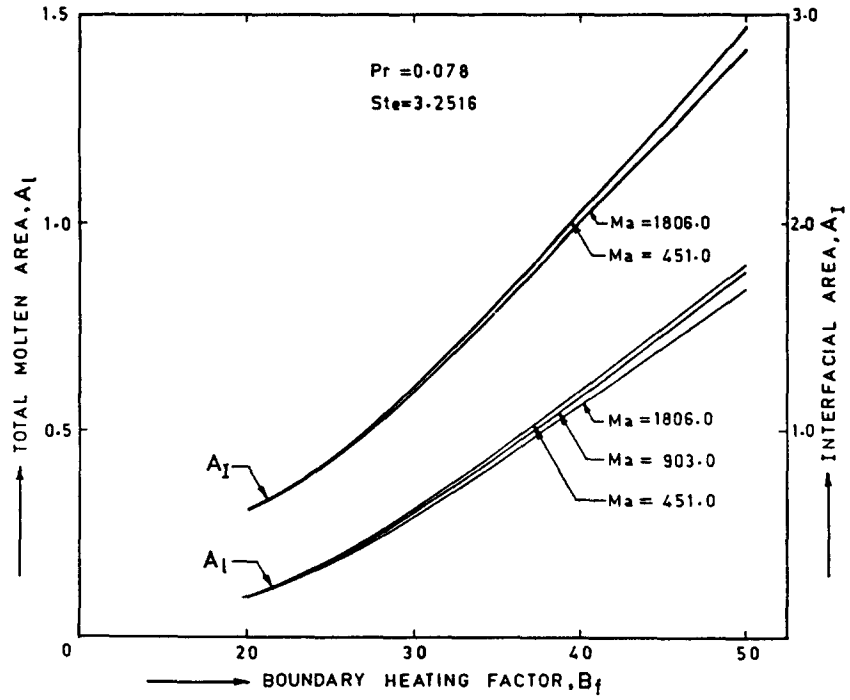

FIG. 10. Variation of total molten area (A_l) and interfacial area (A_I) with Marangoni number (Ma) and boundary heating factor (B_f) for steel.

increases steadily with time and the development of z_{max} is dependent on combined heat transfer—conduction and primary and secondary convection. The development of r_{max}, on the other hand, is controlled by primary convection aided by conduction.

4. CONCLUSIONS

The conclusions of this work may be summarized as follows.

(i) For different metallic systems it is possible to

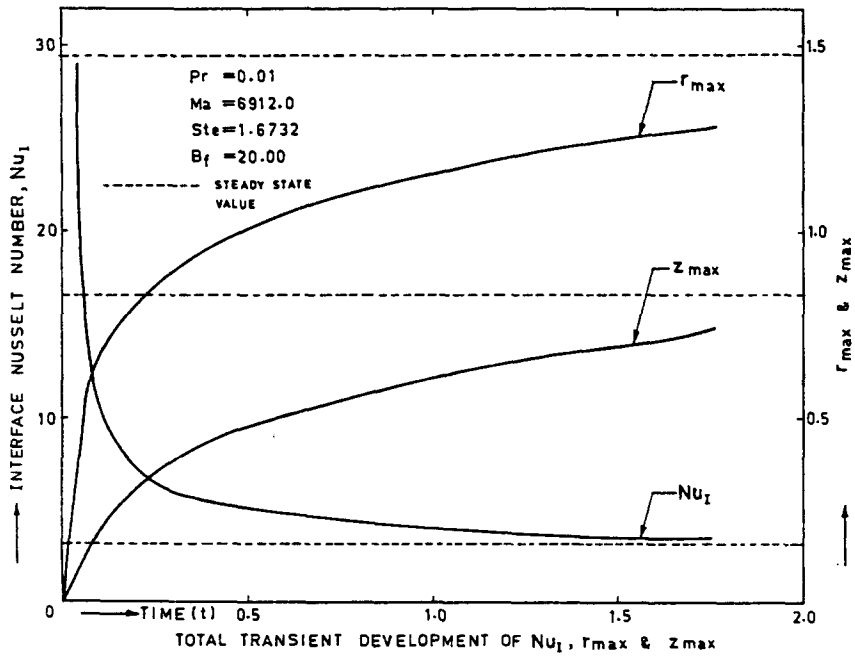

FIG. 11. Variation of interface Nusselt number (Nu_I), r_{max} and z_{max} with time for aluminium with a laser of $q = 4.0 \times 10$ W m^{-2} and $r_0 = 2.0$ mm.

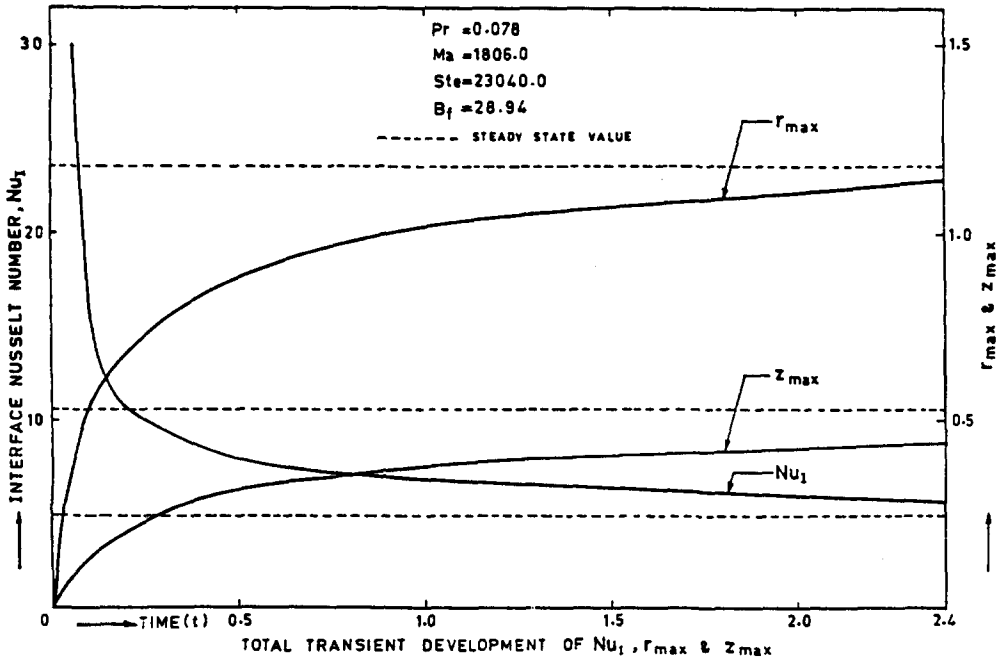

FIG. 12. Variation of interface Nusselt number (Nu_l), r_{max} and z_{max} with time for steel with a laser of $q = 4.0 \times 10^2$ W m^{-2} and $r_0 = 2.0$ mm.

identify a critical value of B_f below which convection is negligible. For steel and aluminium, the critical B_f values are 20.0 and 10.0, respectively.

(ii) The variation of θ_{bulk} with B_f and Ma shows the strong influence of convection at higher B_f values when θ_{bulk} changes slowly with B_f due to better transport of heat in the presence of flow.

(iii) Below the critical value of B_f, both θ_{bulk} and Nu_l remain invariant with the change in Ma, showing conduction to be the dominant form of heat transfer.

(iv) $Nu_{l_{ss}}$ with convection is always higher than $Nu_{l_{ss}}$ without convection, resulting from the higher rate of heat transfer in the presence of convection.

(v) r_{max}/r_0 remains invariant with the change in Ma for a particular B_f value, and thus shows that primary convection increases in proportion to the radius of the beam (r_0) for the same (qr_0).

(vi) Due to the variation in the size and strength of the secondary cells, z_{max}/r_0 decreases with increasing beam radius for a particular power density.

(vii) The interface area A_l and the molten pool area A_l are marginally influenced by Ma, but are strong functions of B_f.

(viii) It is possible to correlate θ_{bulk}, r_{max}, z_{max} and $Nu_{l_{ss}}$ as functions of process parameters B_f, Ma, Pr and Ste. Correlations are derived for steel and aluminium.

Acknowledgements—The authors thank Prof. E. C. Subbarao, Director, Tata Research Development and Design Centre, Pune, for many fruitful discussions. This work was supported by a project from the Department of Science and Technology, New Delhi.

REFERENCES

1. C. Chan, J. Mazumder and M. M. Chen, A two-dimensional model for convection in laser melted pool, *Met. Trans.* **15A**, 2175–2184 (1984).
2. C. Chan, J. Mazumder and M. M. Chen, A model for surface tension flows in laser surface alloying. In *Lasers in Materials Processing* (Edited by E. A. Metzbower), pp. 150–157. American Society of Metals, Metals Park, Ohio (1983).
3. B. Basu and J. Srinivasan, Numerical study of steady state laser melting problem, *Int. J. Heat Mass Transfer* **31**, 2331–2338 (1988).
4. B. Basu and A. W. Date, Numerical study of steady state and transient laser melting problems—I. Characteristics of flow field and heat transfer, *Int. J. Heat Mass Transfer* **33**, 1149–1163 (1990).

ETUDE NUMERIQUE DES PROBLEMES PERMANENTS OU VARIABLE DE FUSION LASER—II. EFFETS DES PARAMETRES DU MECANISME

Résumé—On présente une étude paramétrique des problèmes de fusion laser. Des études sont conduites sur l'acier ($Pr = 0{,}078$) et l'aluminium ($Pr = 0{,}01$) en faisant varier le rayon du faisceau (0,5; 1,0 et 2,0 mm) et la densité de puissance (10^8–10^9 W m^{-2}). Les effets de ces paramètres sur la température moyenne du bain liquide, la largeur et la profondeur du bain, l'aire de l'interface solide/liquide sont étudiés ainsi que sur le nombre de Nusselt. On compare les cas de conduction pure et de convection pour analyser l'effet de convection sur le transfert thermique global et on identifie les valeurs critiques de ces paramètres au dessous desquelles la convection est négligeable. La largeur maximale du bain est invariante pour des faisceaux de différents rayons quand le produit de la puissance du faisceau par le rayon est constant. Des corrélations sont données pour déterminer la température moyenne du liquide, la largeur maximale et la profondeur du bain, ainsi que le nombre de Nusselt en fonction des paramètres.

NUMERISCHE UNTERSUCHUNG VON STATIONÄREN UND INSTATIONÄREN LASERGEHEIZTEN SCHMELZVORGÄNGEN—II. EINFLUSS DER PROZESSPARAMETER

Zusammenfassung—Eine Parameterstudie von Laserschmelzvorgängen wird vorgestellt. Für Stahl ($Pr = 0{,}078$) und Aluminium ($Pr = 0{,}01$) werden der Strahlradius (0,5; 1,0 und 2,0 mm) und die Strahlleistungsdichte (10^8–10^9 W m^{-2}) variiert. Der Einfluß dieser Parameter auf die mittlere Temperatur der Schmelze, die größte Breite und Tiefe der Schmelzzone, die Größe der Grenzfläche zwischen Schmelze und Festkörper, die Größe der Schmelzenoberfläche und die Grenzflächen-Nusselt-Zahl wird untersucht. Es werden vergleichende Studien des Schmelzvorgangs mit reiner Wärmeleitung und reiner Konvektion durchgeführt, um den Einfluß des konvektiven Wärmetransports auf den Gesamtwärmetransport und damit auch die kritischen Werte der Prozeßparameter zu bestimmen, unterhalb derer der konvektive Wärmetransport vernachlässigbar ist. Die maximale Breite der Schmelzzone ist unabhängig vom Strahlradius, wenn das Produkt aus Strahlradius und -leistung konstant ist. Abschließend werden Korrelationen zur Bestimmung der mittleren Temperatur der Schmelze, der maximalen Breite und Tiefe der Schmelzzone und der Grenzflächen-Nusselt-Zahl in Abhängigkeit von den Prozeßparametern hergeleitet.

ЧИСЛЕННОЕ ИССЛЕДОВАНИЕ СТАЦИОНАРНЫХ И НЕСТАЦИОНАРНЫХ ЗАДАЧ ЛАЗЕРНОЙ ПЛАВКИ—II. РОЛЬ ПАРАМЕТРОВ ПРОЦЕССА

Аннотация—Представлено параметрическое исследование задач лазерной плавки. Исследования проведены для случаев стали ($Pr = 0{,}078$) и алюминия ($Pr = 0{,}01$) посредством варьирования радиуса (0,5; 1,0 и 2,0 мм) и плотности мощности (10^8–10^9 Вт · м$^{-2}$) луча. Изучается влияние данных параметров на среднюю массовую температуру жидкости, максимальную ширину и глубину объема расплава, площадь границы раздела твердой и жидкой фаз, площадь жидкой фазы и значение числа Нуссельта на межфазной границе. Для анализа влияния конвекции на общий теплоперенос сравниваются случаи только с кондуктивным и конвективным переносом, и таким образом устанавливаются критические значения параметров процесса, ниже которых конвекция пренебрежимо мала. Найдено, что максимальная ширина объема расплава неизменна при различных радиусах луча и постоянной величине произведения мощности и радиуса луча. Выведены соотношения для определения средней массовой температуры жидкости, максимальной ширины и глубины объема расплава, а также значения числа Нуссельта на межфазной границе по параметрам процесса.